NASA Technical Memorandum 104606, Vol. XX

# Technical Report Series on Global Modeling and Data Assimilation

Max J. Suarez, Editor
*Data Assimilation Office*
*Goddard Space Flight Center*
*Greenbelt, Maryland*

# Volume XX

# Documentation of the Tangent Linear and Adjoint Models of the Relaxed Arakawa-Schubert Moisture Parameterization Package of the NASA GEOS-1 GCM (Version 5.2)

Weiyu Yang
*Supercomputer Computations Research Institute, Florida State University*
I. Michael Navon
*Department of Mathematics and SCRI, Florida State University*
Ricardo Todling
*General Sciences Corporation, Laurel, Maryland*

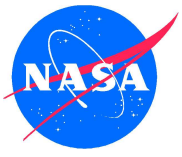


Nasa Aeronautics and
Space Administration
**Goddard Space Flight Center**
Greenbelt, Maryland 20771
**1997**

**Abstract**

A detailed description of the development of the tangent linear model (TLM) and its adjoint model of the Relaxed Arakawa-Schubert moisture parameterization package used in NASA GEOS-1 C-Grid GCM (Version 5.2) is presented. The notational conventions used in the TLM and its adjoint codes are described in detail.

# Contents

# List of Figures

# 1 Introduction

The GEOS-1 C-Grid GCM was developed by the Data Assimilation Office (DAO) at Goddard Laboratory for Atmosphere (GLA), NASA/GSFC (Takacs, et al., 1994; Suarez and Takacs 1994) to be used in conjunction with an analysis scheme to produce a multi-year global atmospheric data set for climate research (Schubert et al., 1993). It has an advanced structure, i.e., a "plug-compatible" structure. It means that if "plug-compatible" rules are followed in coding different GCMs and parameterizations, codes can be "unplugged" from one model and "plugged" into another with little coding effort. Thus each part of the GEOS-1 C-grid GCM can be used independently at another GCM. For instance, the full physics package of GEOS-1 C-grid GCM has been used into NASA/GLA Semi-Lagrangian Semi-Implicit (SLSI) GCM. The DAO and the Climate and Radiation Branch at GLA, NASA/GSFC have produced a library of physical parameterizations and dynamical algorithms which may be utilized for various GCM applications.

There are four physics parameterization packages in the GEOS-1 GCM, i.e., the Relaxed Arakawa-Schubert (RAS) subgrid moisture parameterization and large-scale convection schemes, the shortwave radiation scheme, the longwave radiation scheme, and the turbulence parameterization scheme. Recently, the land surface model (LSM) described by Koster and Suarez (1992) has been fully coupled to the Aries GCM at NASA/GSFC, and the coupled models have been used to address a number of climate-related problems (Koster and Suarez 1996). In the physics packages, the moisture process plays an essential role towards improving the quality of the GCM productions.

In order to obtain a 4-D variational data assimilation system based on the NASA GEOS-1 C-grid GCM including the moisture parameterization process, we need to develop the tangent linear and corresponding adjoint model of this physics package. This document describes the development of the tangent linear and adjoint models of the RAS and large-scale convection schemes as well as the formation of clouds which provides the cloud information used for cloud-radiative interactions.

In Section 2 we provide a condensed description of the moisture parameterization package, including the basic original equations and their discrete forms. Section 3 describes and documents in detail the derivation and coding at the tangent linear model (TLM), and the notational conventions used. Section 4 describes the derivation of the adjoint model code and discusses its validity.

# 2 Description of the Moisture Parameterization Scheme

In a large-scale disturbance, there are many individual cumulus clouds whose spatial and temporal scales are much smaller than the disturbance itself. Because of this scale separa-

tion, it may be possible to predict the time evolution with the collective influence of all the smaller scale cumulus clouds. This is the goal of cumulus parameterization.

Subgrid scale cumulus convection parameterization is a crucial component of any GCMs. Without including it in a GCM, one cannot hope to simulate the right general circulation patterns especially over the tropical region, and some other regions, where cumulus convective activities are frequent and strong.

The necessity of parameterization of cumulus convection was understood and became clear after early research efforts failed to explain theoretically the size and growth rate of tropical cyclones (Lilly 1960; Yanai 1964). Among of the early parameterization researches, Charney and Elisaaen (1964) and Ooyama (1964) presented their classical papers in which the concept of "conditional instability of the second kind" (CISK) was first introduced. CISK describes the cooperative interaction between the cumulus scale and large scale, i.e., the large-scale circulation is responsible for organizing and maintaining cumulus convection by providing the necessary horizontal transport of water vapor, while the cumulus-scale drives the large-scale circulation through the release of latent heat in deep convective elements. CISK mechanism treats cumulus activities to be a function of the large-scale fields and it is now commonly referred to as cumulus parameterization. The simple parameterizations used in these papers led to considerable success in the numerical simulation of tropical cyclones (e.g., Ooyama 1969). Due to the high degree of empiricism and intuition, and the lack of theoretical framework for describing the mutual interaction between a cumulus ensemble and the large-scale environment, these early parameterizations were too crude to be used in GCM.

Ooyama (1971) first proposed a cumulus parameterization theory which took into account the coexistence of a spectrum of clouds. He assumed that cumulus clouds can be represented as non-interacting spherical bubbles, dispatched from the mixed layer. He concluded that the problem of parameterization of cumulus convection reduces to a determination of the dispatch function thus his parameterization scheme is not closed due to the unknown dispatch function.

Before 1974, the basic physical image related to the cumulus parameterization, was that an existing cumulus cloud ensemble produces time changes in the large-scale temperature and moisture fields (Arakawa 1969, 1971, 1972; Betts 1973a, b; Gray 1972; López 1972a, b; Ooyama 1971; Yanai 1971a, b; Yanai et al. 1973). Cumulus convection modifies the large-scale temperature and moisture fields through detrainment and cumulus-induced subsidence in the environment. The detrainment causes large-scale cooling and moistening, and the cumulus-induced subsidence causes large-scale warming and drying. Based on 1956 Marshall Island observation data, Yanai et al. (1973) quantitatively derived these effects from a combination of observed large-scale heat and moisture budget over an area covered by cloud cluster and a cumulus ensemble model which is similar to the one used in Arakawa and Schubert (1974). Their results show the importance of coexistence of shallow clouds

with deep clouds in maintaining the large-scale heat and moisture budgets.

Based on the research results of the cumulus parameterization mentioned above, Arakawa and Schubert (1974, hereafter AS) presented a remarkable achievement, namely they proposed a closed cumulus parameterization theory that describes the mutual interaction of an ensemble of cumulus clouds with the large-scale environment. This is perhaps the most physically complete approach to the issue of cumulus parameterization up to now. The cloud ensemble is represented by a spectrum of idealized model cloud sub-ensembles. Each of the sub-ensembles has its own mass, heat and moisture budget. The vertical transports accomplished by this ensemble of model clouds is ultimately determined by the cloud base mass flux for each member of ensemble. In order to determine this mass flux distribution, Arakawa and Schubert introduced the concept of quasi-equilibrium of the cloud work function, which leads to an integral equation making the cloud base mass flux distribution relating to large-scale thermodynamic processes.

Kuo (1965, 1974) introduced cumulus parameterization for use in tropical cyclone modeling which were subsequently employed in large-scale numerical prediction models (e.g., Krishnamurti 1969; Krishnamurti et al. 1979; the NMC spectral model and the limited-area nonhydrostatic MM5 model). The Kuo parameterization scheme uses different mechanisms to describe physically the scale interaction between the cumulus ensemble and the environment based on similar assumptions comparable to the AS parameterization scheme (Fraedrich 1973). The mechanism applied in the AS scheme is the vertical mass flux relating the fluxes inside and outside a convective element, i.e., the vertical mass transport as the representative variable. Yet the mechanism applied in the Kuo scheme is based on a non-steady deep cumulus model, using the temperature difference between the cumulus cloud and the undisturbed environment and the large-scale convergence of moisture as indicators. The advantage of Kuo's scheme is that, as a parameterization procedure, it provides immediate measures of the cumulus-scale heat and moisture fluxes in terms of measurable large-scale variables, without having to compute cloud dynamical processes (such as entrainment, detrainment and downdrafts) and cloud microphysics processes.

Manabe et al. (1965) introduced an adjustment scheme to simulate subgrid-scale moist convection. Their adjustment includes the dry convective adjustment and the moist convective adjustment. The moist adjustment is performed only when the relative humidity reaches 100% and the lapse rate exceeds the moist adiabatic lapse rate. With these artificial adjustments, they introduced a simplified hydrologic cycle, which consists of the advection of water vapor by large-scale motion, evaporation from the surface, and precipitation process, to simulate the process of moist convection.

The basic closure assumption for the AS parameterization, i.e., the cloud-work function quasi-equilibrium assumption, was examined by Lord and Arakawa (1980). They justified this assumption by considering the kinetic energy budget of a cumulus subensemble. That is, the generation and dissipation of kinetic energy per unit cloud-base mass flux should

approximately balance over time scales of the large-scale processes, and such kinetic energy generation (the cloud-work function) and dissipation per unit cloud-base mass flux for a given subensemble should not depend substantially on the large-scale conditions. They calculated cloud-work functions from a variety of data sets in the tropics and subtropics including the GATE, AMTEX, VIMHEX as well as composited typhoon data. Their results confirmed the correctness of the the cloud-work function quasi-equilibrium assumption. Lord (1982) continued to verify the AS cumulus parameterization using a semi-prognostic approach applied GATE Phase III data. His results show that the calculated precipitation agrees very well with estimates from the observed large-scale moisture budget and from radar observations. The calculated vertical profiles of cumulus warming and drying are also quite similar to the observation. His results also show that the error caused by the cloud-work function quasi-equilibrium assumption is generally less than 10%. In his paper, some additional experiments were also carried out to investigate the sensitivity of the AS scheme to some of the arbitrary parameters and assumptions. After these verifications and investigations, Lord et al. (1982) incorporated the discretized form of the AS scheme into the UCLA GCM.

The AS cumulus parameterization has been widely tested and applied for various purposes. Ramanathan (1980) applied the AS scheme in a semi-prognostic case study of a monsoon depression when it was forming. He found that quasi-equilibrium held even in this disturbed situation, and precipitation and cumulus heating rates were reasonable. Krishnamurti et al. (1980) compared five cumulus parameterization schemes using the semi-prognostic approach. The calculated rainfall rate were compared with the observed estimates from GATE A/B data. Moorthi and Arakawa (1985) used the AS parameterization to carry out a systematic investigation on how cumulus heating affects baroclinic instability. Kao and Ogura (1987) tested the AS scheme through a semi-prognostic approach using the tropical cloud band data and the tropical composite easterly wave disturbance data. They found that cloud heating and drying effects as well as the predicted cloud population agreed rather well with the observations. Sud et al. (1991) tested the AS scheme using the GLA/GCM. They modified some parameters used in the AS scheme to improve parameterization, and found that the role of cumulus convection in maintaining the observed tropical rainfall and 850 mb easterly winds was satisfactory.

Due to the complexity of the original AS cumulus parameterization, some research efforts were carried out aimed at simplified parameterization schemes which would still provide realistic values of the thermal forcing by convection under various synoptic conditions (e.g., Ceselski 1974; Hack et al. 1984; Tiedtke 1989; Moorthi and Suarez 1992). Hack et al. (1984) used a convective flux form of the AS scheme instead of the original detrainment form. This flux form is more convenient to use in numerical weather prediction models. Tiedtke (1989) introduced a much simpler parameterization scheme and compared its results with the conventional convection scheme used in NWP at ECMWF. In 1992, Moorthi and Suarez introduced the "Relaxed Arakawa-Schubert" (RAS) cumulus parameterization scheme which is a simplified AS parameterization scheme. It is very efficient, and produces

results very close to those of the standard AS implementation. The RAS scheme is used in the NASA GEOS-1 GCM and is described in next subsection, following closely Moorthi and Suarez (1992).

## 2.1 Cumulus Parameterization Package of the NASA GEOS-1 GCM

The cumulus parameterization package of the NASA GEOS-1 GCM is the RAS scheme proposed by Moorthi and Suarez (1992). RAS makes two major simplifications in the standard AS implementation:

1) It modifies the entrainment relation to avoid the costly calculation that is required to find the entrainment parameter of clouds detraining at each levels.

2) "Relaxes" the state toward equilibrium instead of requiring "quasi-equilibrium" of the cloud ensemble to be achieved each time the parameterization is invoked.

The iteration method chosen in the RAS scheme considers one cloud type at a time and computes the cumulus mass flux that would be required to maintain the invariance of the work function if there were no other clouds present. It then uses the heating and drying effects of the given type of cloud to change the large-scale environment fields; the same thing is done for another cloud type based on the new modified environment fields. With this procedure, each step is in the direction of a single-cloud equilibrium, but in the course of iteration, all cloud types affect each other by modifying the environment.

*a. Cloud model*

The cloud model used by RAS is a simplified form of that in the AS scheme. The first major simplification introduced is to assume that the normalized mass flux for each cloud type is a linear function of height instead of the exponential function used in AS. Thus

$$\frac{\partial \eta_\lambda(z)}{\partial z} = \lambda \tag{1}$$

where $\eta_\lambda(z)$ is the normalized mass flux for cloud type $\lambda$ at height $z$, with boundary condition

$$\eta_\lambda(z_B) = 1 \tag{2}$$

The hydrostatic equation is used in the form

$$\frac{\partial z}{\partial P} = -\frac{c_p}{g}\theta \tag{3}$$

where $P = (p/p_0)^{R/c_p}$, $p$ is the pressure, $R$ is the gas constant, $c_p$ is the specific heat at constant pressure, $g$ is the gravitational acceleration, $\theta$ is the potential temperature, and

$p_0 = 1000\ mb$. From Eqs. (3) and (1), we have

$$\frac{\partial \eta_\lambda(P)}{\partial P} = -\frac{c_p}{g}\theta\lambda \tag{4}$$

and integration gives

$$\eta_\lambda(P) = 1 + \frac{c_p}{g}\lambda \int_P^{P_B} \theta \ dP \tag{5}$$

where $P_B \equiv P(z_B)$, is the pressure at the cloud base height.

As in the AS scheme, the large-scale budget of moist static energy and total water substance for each cloud type are

$$\frac{\partial}{\partial P}\left[\eta_\lambda(P) h^c_\lambda(P)\right] = \frac{\partial \eta_\lambda(P)}{\partial P} h(P) \tag{6}$$

and

$$\frac{\partial}{\partial P}\left\{\eta_\lambda(P)\left[q^c_\lambda(P) + l^c_\lambda(P)\right]\right\} = \frac{\partial \eta_\lambda(P)}{\partial P} q(P) \tag{7}$$

where $h^c_\lambda(P)$, $q^c_\lambda(P)$, and $l^c_\lambda(P)$ are the cloud moist static energy, specific humidity, and liquid water mixing ratio for cloud type $\lambda$ at level $P$, respectively. $h(P)$ and $q(P)$ are the moist static energy and specific humidity in the environment, respectively.

In Eq. (7), the precipitation term has been neglected for simplicity. It is assumed that all liquid water is carried to the cloud top where part is precipitated and part is evaporated, depending on the cloud type. Since the liquid water loading and the precipitation effects are excluded from Eq. (7), there is no need to specify the vertical distribution of the precipitation and of the liquid water.

With these assumptions, the detrainment level of the cloud type $\lambda$ is the level at which the moist static energy within clouds equals the saturation moist static energy of the environment. That is

$$h^c_\lambda(P_D) = h^*(P_D) \tag{8}$$

where $P_D = P_D(\lambda)$ is the detrainment level.

Integrating Eq. (6) from $P_B$ to $P_D$, we obtain

$$\eta_\lambda(P_D) h^c_\lambda(P_D) - h_B = -\frac{c_p}{g}\lambda \int_{P_B}^{P_D} \theta h(P) \ dP \tag{9}$$

Combining Eqs. (5) and (9), Eq. (8) can be solved directly for the value $\lambda$ corresponding to clouds that detrain at a given level $P_D$:

$$\lambda(P_D) = \frac{h_B - h^*(P_D)}{\frac{c_p}{g}\int_{P_D}^{P_B} \theta(P)\left[h^*(P_D) - h(P)\right] \ dP} \tag{10}$$

Similarly, assuming the cloud air is saturated at the level of non-buoyancy,

$$q_\lambda^c(P_D) = q^*(P_D) \tag{11}$$

and integrating Eq. (7) from $P_D$ to $P_B$, the liquid water mixing ratio at the detrainment level $l(P_D)$ is calculated from

$$l(P_D) \equiv l_\lambda^c(P_D) = \frac{1}{\eta_\lambda(P_D)} \times \left[ q(P_B) + \frac{c_p}{g}\lambda \int_{P_D}^{P_B} \theta q(P)\ dP \right] - q^*(P_D) \tag{12}$$

*b. Cloud work function*

Following AS and neglecting the effects of water vapor and liquid water on the buoyancy, the cloud work function $A_\lambda$ is

$$A_\lambda = \int_{z_B}^{z_D} \frac{g}{c_p \overline{T(z)}} \eta_\lambda(z)[s_\lambda^c(z) - s(z)]\ dz \tag{13}$$

for cloud type $\lambda$, where $\overline{T(z)}$ is the temperature in the environment at height $z$, and $s_\lambda^c(z)$ and $s(z)$ are the cloud's and the environment's dry static energies, respectively.

Using the hydrostatic equation (3), we have

$$A_\lambda = \int_{P_D}^{P_B} \eta_\lambda(P) \frac{[s_\lambda^c(P) - s(P)]}{P}\ dP \tag{14}$$

To obtain the cloud work function in terms of the moist static energy, let us approximate the static energy difference as

$$s_\lambda^c(P) - s(P) \approx \frac{1}{1+\gamma(P)}[h_\lambda^c(P) - h^*(P)] \tag{15}$$

where $\gamma(P) = (L/c_p)[dq^*(P)/dT]$, $L$ is the latent heat of condensation of water vapor and $h^*$ and $q^*$ are the saturation moist static energy energy and the saturation specific humidity of the environment. Finally the work function form used in the GCM is

$$A_\lambda = \int_{P_D}^{P_B} \frac{\eta_\lambda(P)}{1+\gamma(P)} \frac{h_\lambda^c(P) - h^*(P)}{P}\ dP \tag{16}$$

*c. Cumulus effects on the large-scale budgets*

The rate of change of dry and moist static energies due to cumulus convection can be written in the form

$$\left(\frac{\partial s}{\partial t}\right)_c = gM_c\frac{\partial s}{\partial p} - gLD(P)l(P)[1 - r(P)] \tag{17}$$

and

$$\left(\frac{\partial h}{\partial t}\right)_c = gM_c\frac{\partial h}{\partial p} - gD(P)(h^* - h) \tag{18}$$

where $M_c(P)$ is the total cumulus mass flux per unit horizontal area at level $P$, $D(P)$ is the detrained mass per unit area and unit pressure depth, and $r(P)$ is the fraction of the detrained liquid water which is precipitated. In the NASA GEOS-1 GCM (version 5.2), $r(P)$ is calculated by

$$r(P) = M_B(\lambda)l(P_D) \tag{19}$$

$M_c(P)$ involves contributions from all cloud types penetrating level $P$, i.e.,

$$M_c(P) = \int_0^{\lambda(P)} \eta_\lambda(P)m_B(\lambda)\ d\lambda \tag{20}$$

where $\lambda(P)$ is given by Eq. (10), and $m_B(\lambda)$ is the cloud-base mass flux per unit $\lambda$. The mass detrainment rate

$$D(P) = \eta_\lambda(P)m_B(\lambda)\frac{d\lambda(P)}{dp} \tag{21}$$

In the NASA GEOS-1 GCM, the continuous spectrum of clouds is divided into subensembles of finite $\Delta\lambda$ and the effects of each subensemble are considered independently. Thus for the $i$th spectral band (from $\lambda_i - \Delta\lambda_i$ to $\lambda_i$), we have

$$M_c^i(P) = \begin{cases} \int_{\lambda_i-\Delta\lambda_i}^{\lambda_i} \eta_\lambda(P)m_B(\lambda)\ d\lambda, & P > P_D(\lambda_i), \\ \int_{\lambda_i-\Delta\lambda_i}^{\lambda(P)} \eta_\lambda(P)m_B(\lambda)\ d\lambda, & P_D(\lambda_i) \geq P \geq P_D(\lambda_i - \Delta\lambda_i), \\ 0, & \text{otherwise} \end{cases} \tag{22}$$

and

$$D^i(P) = \begin{cases} \eta_\lambda(P)m_B(\lambda)\frac{d\lambda}{dp}, & P_D(\lambda_i) \geq P \geq P_D(\lambda_i - \Delta\lambda_i), \\ 0, & \text{otherwise} \end{cases} \tag{23}$$

where $P_D(\lambda_i)$ is the detrainment level of clouds with $\lambda = \lambda_i$. It may be obtained by solving Eq. (10).

When $\lambda_i$ is small, we may assume that $m_B(\lambda) \simeq m_B(\lambda_i)$, thus neglecting terms in $(\Delta\lambda_i)^2$, Eq. (22) becomes

$$M_c^i(P) = \begin{cases} \eta_{\lambda_i}(P)m_B(\lambda_i)\Delta\lambda_i, & P > P_D(\lambda_i), \\ \eta_{\lambda_i}(P)m_B(\lambda_i)[\lambda(P) - \lambda_i + \Delta\lambda_i], & P_D(\lambda_i) \geq P \geq P_D(\lambda_i - \Delta\lambda_i), \\ 0, & \text{otherwise} \end{cases} \tag{24}$$

Similarly, approximating the $d\lambda/dp$ in Eq. (23) by $\Delta\lambda_i[p_D(\lambda_i) - p_D(\lambda_i - \Delta\lambda_i)]^{-1}$, we have

$$D^i(P) = \begin{cases} \eta_{\lambda_i}(P)m_B(\lambda_i)\Delta\lambda_i[p_D(\lambda_i) - p_D(\lambda_i - \Delta\lambda_i)]^{-1}, & P_D(\lambda_i) \geq P \geq P_D(\lambda_i - \Delta\lambda_i), \\ 0, & \text{otherwise} \end{cases} \tag{25}$$

Then Eqs. (17) and (18) can be rewritten as

$$\left(\frac{\partial s}{\partial t}\right)_c = \Gamma_s(P) m_B(\lambda_i) \Delta\lambda_i \tag{26}$$

and

$$\left(\frac{\partial h}{\partial t}\right)_c = \Gamma_h(P) m_B(\lambda_i) \Delta\lambda_i \tag{27}$$

where

$$\Gamma_s(P) = \begin{cases} g\eta_{\lambda_i}(P)\frac{\partial s}{\partial p}, & p > p_D(\lambda_i), \\ g\eta_{\lambda_i}(P)[\lambda(P) - \lambda_i + \Delta\lambda_i](\Delta\lambda_i)^{-1}\frac{\partial s}{\partial p} & \\ +g\eta_{\lambda_i}(P)[p_D(\lambda_i) - p_D(\lambda_i - \Delta\lambda_i)]^{-1} & \\ \times l_{\lambda_i}(P_D) L[1 - r(P_D)], & p_D(\lambda_i) \geq p \geq p_D(\lambda_i - \Delta\lambda_i), \\ 0, & \text{otherwise} \end{cases} \tag{28}$$

and

$$\Gamma_h(P) = \begin{cases} g\eta_{\lambda_i}(P)\frac{\partial h}{\partial p}, & p > p_D(\lambda_i), \\ g\eta_{\lambda_i}(P)[\lambda(P) - \lambda_i + \Delta\lambda_i](\Delta\lambda_i)^{-1}\frac{\partial h}{\partial p} & \\ +g\eta_{\lambda_i}(P)[p_D(\lambda_i) - p_D(\lambda_i - \Delta\lambda_i)]^{-1} & \\ \times [h^*(P_D) - h(P_D)], & p_D(\lambda_i) \geq p \geq p_D(\lambda_i - \Delta\lambda_i), \\ 0, & \text{otherwise} \end{cases} \tag{29}$$

Finally, the rate of change of the large-scale prognostic variables, the potential temperature and specific humidity due to the $i$th cloud subensemble can be written as

$$\left(\frac{\partial \theta}{\partial t}\right)_c = \frac{m_B(\lambda_i)\Delta\lambda_i}{c_p P}\Gamma_s(P) \tag{30}$$

and

$$\left(\frac{\partial q}{\partial t}\right)_c = \frac{1}{L} m_B(\lambda_i)\Delta\lambda_i[\Gamma_h(P) - \Gamma_s(P)] \tag{31}$$

*d. Mass-flux kernel and cloud-base mass flux*

In AS, the change rate of cloud work function is expressed as

$$\frac{dA_\lambda}{dt} = \left(\frac{dA_\lambda}{dt}\right)_c + \left(\frac{dA_\lambda}{dt}\right)_{ls} \tag{32}$$

where the subscripts $c$ and $ls$ denote the contributions from the cloud-scale and the large-scale processes, respectively.

From Eq. (16) and together with some assumptions, i.e., the time variations of pressures at the cloud base and top equal to zero, ignoring the time dependence of $\theta$ in Eq. (5), and using

$$\frac{\partial h^*(P)}{\partial t} \approx [1 + \gamma(P)]\frac{\partial s(P)}{\partial t} \tag{33}$$

the change rate of cloud work function in terms of the rate of change of the large-scale variables, $h$ and $s$, can be approximately obtained as

$$\frac{dA_\lambda}{dt} = \int_{P_D}^{P_B} \frac{dP}{P[1+\gamma(P)]}$$
$$\times \left\{ \frac{\partial h(P_B)}{\partial t} - [1+\gamma(P)]\frac{\partial s(P)}{\partial t} + \frac{c_p}{g}\lambda \int_P^{P_B} \theta \left( \frac{\partial h(P')}{\partial t} - [1+\gamma(P)]\frac{\partial s(P)}{\partial t} \right) dP' \right\} \quad (34)$$

In AS, the cloud-scale contributions on $dA_\lambda/dt$ is

$$\left(\frac{dA_\lambda}{dt}\right)_c = \int_0^{\lambda_{max}} K_{\lambda,\lambda'} m_B(\lambda')\, d\lambda' \quad (35)$$

where the kernel $K_{\lambda,\lambda'}$ represents the rate of change of the cloud work function of cloud type $\lambda$ per unit cloud-base mass flux of cloud type $\lambda'$. These are not direct cloud-cloud interactions, but indirect effects of the various cloud types on each other through their environment. For quasi equilibrium to hold for the cumulus ensemble as a whole, these interactions must occur quickly compared to changes in the large-scale forcing. The standard implementation assumes that they occur instantaneously, resulting in a quasi-static balance between the cloud ensemble and the large-scale forcing. It is this assumption that results in an ill-posed problem, with the possibility that either no mass-flux distribution can produce an exact balance for all clouds with positive buoyancy or that (most frequently) multiple distributions can satisfy an "overadjustment" problem (Silva-Dias and Schubert 1977) in which some of the possible cloud types are overstabilized by the effects of other cloud types.

The main assumption of RAS is that the interaction between clouds, represented by the off-diagonal terms of $K$ in Eq. (35), occurs over a short but finite time and that at any instant the computations for each cloud and each cloud type are just based on the "current" environment which already has been affected by influences of some other type of cumulus convections. In this way, the cloud interactions are taken into account. The ill-posedness of the original AS implementation is thus removed by solving an initial value problem that selects an equilibrium distribution that depends on the time scales specified for the adjustment of the individual cloud types. In RAS, considering the effects of a single subensemble on the cloud work function, Eq. (35) reduces to

$$K_{\lambda_i,\lambda_i} = \frac{1}{m_B(\lambda_i)\Delta\lambda_i} \left(\frac{dA_{\lambda_i}}{dt}\right)_c \quad (36)$$

Finally, from Eqs. (34), (26) and (27), the approximate $K_{\lambda_i,\lambda_i}$ is given by

$$K_{\lambda_i,\lambda_i} = \int_{P_D}^{P_B} \frac{dP}{P[1+\gamma(P)]} \times$$
$$\left\{ \Gamma_h(P_B) - [1+\gamma(P)]\Gamma_s(P) + \frac{c_p}{g}\lambda_i \int_P^{P_B} \theta \left( \Gamma_h(P') - [1+\gamma(P)]\Gamma_s(P) \right) dP' \right\} \quad (37)$$

The subensemble cloud-base mass flux $m_B(\lambda_i)\Delta\lambda_i$ is obtained by equating the large-scale and cloud-scale changes of $A$, i.e., making $dA_{\lambda_i}/dt = 0$, we have

$$m_B(\lambda_i)\Delta\lambda_i = \begin{cases} -\left(\frac{dA_{\lambda_i}}{dt}\right)_{ls} K^{-1}_{\lambda_i,\lambda_i}, & m_B(\lambda_i) > 0, \\ 0, & \text{otherwise.} \end{cases} \tag{38}$$

In the GEOS-1 GCM, the large-scale forcing $(dA_{\lambda_i}dt)_{ls}$ is calculated directly from time difference:

$$\left(\frac{dA_{\lambda_i}}{dt}\right)_{ls} = \frac{A_{\lambda_i}(t+\Delta t) - A_{\lambda_i}(t)}{\Delta t} \tag{39}$$

where $A_{\lambda_i}(t+\Delta t)$ is the cloud work function calculated from the profiles of $\theta$ and $q$ after they are modified by the large-scale processes over a time interval $\Delta t$. This is a good approximation as long as $\Delta t$ is small. In the GCM, $A_{\lambda_i}(t+\Delta t)$ is replaced by the value of the cloud work function after modification of the environment by large-scale effects and using a cloud-type dependent critical value of the work function instead of $A_{\lambda_i}(t)$. Due to the convective parameterization is designed to nearly neutralize the instability, the critical value of the work function is near zero.

In RAS, the cloud type is determined by the height of cloud-top level and the kernel is computed explicitly since only the diagonal elements are required.

In addition to RAS scheme, GEOS-1 GCM employs a Kessler-type scheme for the re-evaporation of falling rain (Sud and Molod 1988). The scheme accounts for the rainfall intensity, the drop size distribution, and the temperature, pressure and relative humidity of the surrounding air.

Due to the increased vertical resolution in the planetary boundary layer (PBL), the lowest two model layers are averaged to provide the sub-cloud layer for RAS (about 50 mb thick). Each time RAS is invoked (every ten simulated minutes), the possibility for shallow convection is checked for the two layers just above the cloud base. RAS also randomly chooses ten other cloud-top levels for the possibility of convection, from just above the cloud base to the model top layer.

Supersaturation or large-scale convection is defined in the GEOS-1 GCM whenever the specific humidity in any grid point exceeds its supersaturation value. The large-scale precipitation scheme rains at supersaturation, and re-evaporates during descent to partially saturate lower layers in a process that accounts for some simple microphysics.

Convective and large-scale cloudiness which is used for cloud-radiative interactions are determined diagnostically as part of the cumulus and large-scale parameterizations. The convective and large-scale cloud fractions are combined into two separate arrays for use in the shortwave and longwave radiation packages.

Supersaturation or large-scale cloudiness is defined whenever the large-scale precipitation scheme determines that the grid box at any level becomes supersaturated. In order to ensure

that at any instant the total cloud fraction is less than or equal to one, supersaturation clouds are only prescribed when there are no deep convective clouds.

Since in the current moist version of GEOS-1 GCM which includes just the moist process, in the tangent linear model and its adjoint code the cloud formation part is not employed (i.e., all the related lines are commended out) although this part of code has already been included.

## 2.2 Description of the Discretization of the Moisture Physics Parameterization

*a. Cloud model*

All clouds are assumed to have the same base. We will refer to that cloud type with its detrainment level in layer $i$, as the $i$th cloud type.

The normalized mass flux for each cloud type is a linear function of height,

$$\eta_{i,k-1/2} - \eta_{i,k+1/2} = \lambda_i (Z_{k-1/2} - Z_{k+1/2}), \qquad k = i+1, i+2, ..., K-1 \tag{40}$$

where $\eta_{i,k+1/2}$ is the cloud mass flux of the $i$th cloud type at level $k+1/2$ normalized by its value at the cloud base, $\lambda_i$ is its entrainment rate, and $Z_{k+1/2}$ is the height of level $k+1/2$. Equation (40) applies from the layer immediately below the detrainment layer to the layer immediately above the cloud base which is at $K-1/2$. We assume the detrainment occurs at the middle of the detrainment layer and therefore that there is an additional half-layer at the top over which the cloud entrains,

$$\eta_{i,i} - \eta_{i,i+1/2} = \lambda_i (Z_i - Z_{i+1/2}) \tag{41}$$

The vertical coordinate is specified by the pressure at the half-integer levels ($p_{k+1/2}$, $k = 1, 2, ..., K$). The discrete form of hydrostatic equation over the full layers is,

$$Z_{k-1/2} - Z_{k+1/2} = \frac{c_p}{g} \theta_k (P_{k+1/2} - P_{k-1/2}), \qquad k = 1, 2, ..., K \tag{42}$$

For the hydrostatic equation over the lower half of each layer,

$$Z_k - Z_{k+1} = \frac{c_p}{g} \theta_{k+1/2} (P_{k+1} - P_k). \qquad k = 1, 2, ..., K \tag{43}$$

$\theta$ is the potential temperature, and $P$ is the form as

$$P_{k+1/2} = (p_{k+1/2}/p_0)^{\kappa} \tag{44}$$

and

$$P_k = \frac{1}{1+\kappa} \left( \frac{P_{k+1/2} p_{k+1/2} - P_{k-1/2} p_{k-1/2}}{p_{k+1/2} - p_{k-1/2}} \right) \tag{45}$$

which is the form suggested by Phillips (1974) and used in Arakawa and Suarez (1983). Here $\kappa \equiv R/c_p$.

From Eqs. (40) to (42), we have

$$\eta_{i,k-1/2} - \eta_{i,k+1/2} = \beta_k \theta_k \lambda_i, \qquad k = i+1, i+2, ..., K-1 \tag{46}$$

where

$$\beta_k = \frac{c_p}{g}(P_{k+1/2} - P_{k-1/2}) \tag{47}$$

For the last half-layer up to the detrainment level,

$$\eta_{i,i} = \eta_{i,i+1/2} + \beta_i \theta_i \lambda_i \tag{48}$$

where

$$\beta_i = \frac{c_p}{g}(P_{i+1/2} - P_i) \tag{49}$$

Summing Eq. (46) and combining with Eq. (48), we obtain the normalized mass flux at the detrainment level,

$$\eta_{i,i} = 1 + \lambda_i \sum_{k=K-1}^{i} \beta_k \theta_k \tag{50}$$

where $\eta_{i,K-1/2} = 1$ is used.

The discrete form of the moist static energy budget of each cloud type is

$$\begin{aligned} \eta_{i,k-1/2} h^c_{i,k-1/2} - \eta_{i,k+1/2} h^c_{i,k+1/2} = \quad & (\eta_{i,k-1/2} - \eta_{i,k+1/2}) h_k, \\ & k = i+1, i+2, ..., K-1 \end{aligned} \tag{51}$$

where $h_k$ is the environment moist static energy of layer $k$, $h^c_{i,k+1/2}$ is the cloud moist static energy of the $i$th cloud type at level $k+1/2$. For the half-layer at the cloud top we have

$$\eta_{i,i} h^c_{i,i} - \eta_{i,i+1/2} h^c_{i,i+1/2} = (\eta_{i,i} - \eta_{i,i+1/2}) h_i \tag{52}$$

Summing Eq. (51) and combining Eq. (52), we obtain the cloud-top moist static energy expression as

$$\eta_{i,i} h^c_{i,i} = h_K + \sum_{j=K-1}^{i+1} \left[ (\eta_{i,j-1/2} - \eta_{i,j+1/2}) h_j \right] + (\eta_{i,i} - \eta_{i,i+1/2}) h_i \tag{53}$$

Ignoring precipitation, the cloud total water is

$$\begin{aligned} \eta_{i,k-1/2}(q^c_{i,k-1/2} + l_{i,k-1/2}) \quad - \quad & \eta_{i,k+1/2}(q^c_{i,k+1/2} + l_{i,k+1/2}) = (\eta_{i,k-1/2} - \eta_{i,k+1/2}) q_k, \\ & k = i+1, i+2, ..., K-1 \end{aligned} \tag{54}$$

where $q^c_{i,k+1/2}$ and $l_{i,k+1/2}$ are the specific humidity and the liquid water mixing ratio of the $i$th cloud type at level $k+1/2$. The rhs of Eq. (54) assumes no liquid water in the

environment. Assuming $q^c_{i,i} = q^*_i$, where $q^*_i$ is the saturation specific humidity of layer $i$, we obtain,

$$l_{i,i} = \frac{1}{\eta_{i,i}} \left[ q_K + \sum_{j=K-1}^{i+1} \left[ (\eta_{i,j-1/2} - \eta_{i,j+1/2}) q_j \right] + (\eta_{i,i} - \eta_{i,i+1/2}) q_i \right] - q^*_i \tag{55}$$

where $l_{i,i}$ is the liquid water mixing ratio of the detraining air for the $i$th cloud type. Since $\theta$ and $q$ are known and the saturation specific humidity can be calculated and $l_{i,i}$ can be calculated if $\lambda_i$ is known.

Assuming at the detrainment layer

$$h^c_{i,i} = h^*_i \tag{56}$$

where $h^*_i$ is the saturation moist static energy of layer $i$. In the AS, Eq. (56) is a polynomial in $\lambda_i$ whose degree depends on the height of the detrainment level. From Eqs. (40), (41), (53) and (56), the expression for $\lambda_i$ is obtained as

$$\lambda_i = \frac{h_K - h^*_i}{\sum_{j=K-1}^{i} \beta_j \theta_j (h^*_i - h_j)} \tag{57}$$

*b. Cloud work function*

The discrete form of the cloud work function is obtained by discretizing Eq. (16) as

$$\begin{aligned} A_i = & \sum_{j=K-1}^{i+1} \Big[ \epsilon_j \eta_{i,j+1/2} (h^c_{i,j+1/2} - h^*_j) \\ & + \mu_j \eta_{i,j-1/2} (h^c_{i,j-1/2} - h^*_j) \Big] + \epsilon_i \eta_{i,i+1/2} (h^c_{i,i+1/2} - h^*_i) \end{aligned} \tag{58}$$

where $A_i$ is the cloud work function for the $i$th cloud type and $\epsilon$ and $\mu$ are defined as

$$\epsilon_j \equiv \frac{P_{j+1/2} - P_j}{P_j (1 + \gamma_j)}, \qquad j = 1, 2, ..., K-1 \tag{59}$$

and

$$\mu_j \equiv \frac{P_j - P_{j-1/2}}{P_j (1 + \gamma_j)}, \qquad j = 1, 2, ..., K-1 \tag{60}$$

Using Eq. (51) to eliminate $h^c$, the cloud work function can finally be written in terms of environmental quantities as:

$$\begin{aligned} A_i = & \epsilon_{K-1} h_K - \epsilon_i \eta_{i,i+1/2} h^*_i \\ & + \sum_{k=K-1}^{i+1} (\epsilon_{k-1} + \mu_k) \left[ h_K + \sum_{j=K-1}^{k} \left[ (\eta_{i,j-1/2} - \eta_{i,j+1/2}) h_j \right] \right] \\ & - \sum_{k=K-1}^{i+1} \left[ \epsilon_k \eta_{i,k+1/2} + \mu_k \eta_{i,k-1/2} \right] h^*_k \end{aligned} \tag{61}$$

*c. Cumulus effects on the large-scale budgets*

The cumulus effects on the budgets of dry and moist static energies of the environment are discretized as

$$\left(\frac{\partial s_k}{\partial t}\right)_c = \frac{g}{\Delta p_k}\left[M_{k-1/2}(s_{k-1/2} - s_k) + M_{k+1/2}(s_k - s_{k+1/2}) - D_k l_k L(1 - r_k)\right] \tag{62}$$

and

$$\left(\frac{\partial h_k}{\partial t}\right)_c = \frac{g}{\Delta p_k}\left[M_{k-1/2}(h_{k-1/2} - h_k) + M_{k+1/2}(h_k - h_{k+1/2}) + D_k(h_k^* - h_k)\right] \tag{63}$$

where $(\partial s_k/\partial t)_c$ and $(\partial h_k/\partial t)_c$ are the rate of change of dry and moist static energies of layer $k$, $M_{k+1/2}$ is the cumulus mass flux at level $k+1/2$, $D_k$ is the detrained mass at level $k$ and $\Delta p_k = p_{k+1/2} - p_{k-1/2}$. The last term on the rhs of Eq. (62) represents cooling from the re-evaporation of liquid water detrained to the environment. Here $l_k$ is the liquid water mixing ratio, $r_k$ is a cloud-type-dependent precipitation fraction.

In AS implementation, $M_{k+1/2}$ would be the total mass flux of all cloud types penetrating the level $k+1/2$. However in RAS, only one cloud type is considered at a time, then $M_{k+1/2}$ has the form

$$M_{k+1/2} = \begin{cases} M_B(i)\eta_{i,k+1/2}, & i < k, \\ 0, & i \geq k, \end{cases} \tag{64}$$

and

$$D_k = \begin{cases} M_B(i)\eta_{i,i}, & i = k, \\ 0, & i \neq k, \end{cases} \tag{65}$$

Also $l_k = l_{i,i}$, for $i = k$, and $l_k = 0$ otherwise. Eqs. (62) and (63) can be rewritten as

$$\left(\frac{\partial s_k}{\partial t}\right)_c = M_B(i)\Gamma_s(k) \tag{66}$$

and

$$\left(\frac{\partial h_k}{\partial t}\right)_c = M_B(i)\Gamma_h(k) \tag{67}$$

where

$$\Gamma_s(k) = \begin{cases} \frac{g}{\Delta p_k}\left[\eta_{i,k-1/2}(s_{k-1/2} - s_k) + \eta_{i,k+1/2}\right. \\ \left.\times(s_k - s_{k+1/2}) - \eta_{i,i} l_{i,i} L(1 - r_i)\delta_i^k\right], & k = i, i+1, ..., K, \\ 0, & k = 1, 2, ..., i-1 \end{cases} \tag{68}$$

and

$$\Gamma_h(k) = \begin{cases} \frac{g}{\Delta p_k}\left[\eta_{i,k-1/2}(h_{k-1/2} - h_k) + \eta_{i,k+1/2}\right. \\ \left.\times(h_k - h_{k+1/2}) + \eta_{i,i}(h_i^* - h_i)\delta_i^k\right], & k = i, i+1, ..., K, \\ 0, & k = 1, 2, ..., i-1 \end{cases} \tag{69}$$

where $\delta_i^k$ is the Kronecker delta function and it is assumed that $\eta_{i,i-1/2} = \eta_{i,K+1/2} = 0$. Finally the rate of change of potential temperature and specific humidity due to the $i$th cloud type can be obtained as

$$\left(\frac{\partial \theta_k}{\partial t}\right)_c = \frac{M_B(i)}{c_p P_k}\Gamma_s(k), \qquad k = 1, 2, ..., K \tag{70}$$

and

$$\left(\frac{\partial q_k}{\partial t}\right)_c = \frac{1}{L}M_B(i)[\Gamma_h(k) - \Gamma_s(k)], \qquad k = 1, 2, ..., K \tag{71}$$

*d. Mass-flux kernel and cloud-base mass flux*

In RAS, for a single cloud type, only the diagonal element $K_{i,i}$ is required, which is given by

$$K_{i,i} = \frac{1}{M_B(i)}\left(\frac{dA_i}{dt}\right)_c \tag{72}$$

Using the approximate relation

$$\frac{\partial h_k^*}{\partial t} = (1 + \gamma_k)\frac{\partial s_k}{\partial t} \tag{73}$$

and Eqs. (57), (61), (66), (67),

$$\begin{aligned} K_{i,i} = \quad & (\epsilon_{K-1} + \vartheta)\Gamma_h(K) - (\epsilon_i \eta_{i,i+1/2} + \vartheta \eta_{i,i})(1 + \gamma_i)\Gamma_s(i) \\ + \quad & \sum_{k=K-1}^{i+1} \left\{ (\epsilon_{k-1} + \mu_k) \left[ \Gamma_h(K) + \sum_{j=K-1}^{k} (\eta_{i,j-1/2} - \eta_{i,j+1/2})\Gamma_h(j) \right] \right. \\ + \quad & \left. \vartheta(\eta_{i,k-1/2} - \eta_{i,k+1/2})\Gamma_h(k) \right\} + \vartheta(\eta_{i,i} - \eta_{i,i+1/2})\Gamma_h(i) \\ - \quad & \sum_{k=K-1}^{i+1} (\epsilon_k \eta_{i,k+1/2} + \mu_k \eta_{i,k-1/2})(1 + \gamma_k)\Gamma_s(k), \end{aligned} \tag{74}$$

where

$$\begin{aligned} \vartheta = \quad & -\epsilon_i h_i^* \eta_{i,i+1/2} \\ + \quad & \sum_{k=K-1}^{i+1} (\epsilon_{k-1} + \mu_k) \left[ \sum_{j=K-1}^{k} (\eta_{i,j-1/2} - \eta_{i,j+1/2}) h_j \right] \\ - \quad & \sum_{k=K-1}^{i+1} \left[ \epsilon_k \eta_{i,k+1/2} + \mu_k \eta_{i,k-1/2} \right] h_k^* \\ + \quad & \epsilon_i h_i^* + \sum_{k=K-1}^{i+1} (\epsilon_k + \mu_k) h_k^*, \end{aligned} \tag{75}$$

For simplicity, the rate of change of $\epsilon$ and $\mu$ have been ignored. The rate of change of $\lambda_i$ is included through the terms involving $\vartheta$.

With the quasi-equilibrium of cloud work function we obtain,

$$M_B(i) = -\left(\frac{dA_i}{dt}\right)_{ls} K_{i,i}^{-1} \tag{76}$$

when the rhs of Eq. (76) is positive, otherwise $M_B(i) = 0$. The large-scale forcing of the $i$th cloud type $\left(\frac{dA_i}{dt}\right)_{ls}$ can be calculated by Eq. (39). Once $M_B(i)$ is known, the cumulus-induced changes in $\theta$ and $q$ can be calculated.

In RAS, we assume that all liquid water formed inside a cloud is carried to the top detrainment level (i.e., $l_{i,i}$ in Eq. (55)), and a fraction of this detrained liquid water is precipitated and the rest is evaporated within the detrainment layer. Another assumption is the precipitation simply falls to the ground without evaporation. Thus the precipitation $R_i$ for the $i$th cloud type can be written as

$$R_i = M_B(i) r_i l_{i,i} \tag{77}$$

The cloud-type-dependent parameter $r_i$ is set to one for every cloud type in the NASA GEOS-1 GCM Version 5.2.

# 3 Tangent Linear Model of the Moist Process Physics Package

The linearized discrete RAS parameterization equations (40) - (77) are derived as follows. We use $\{\}$ to describe the basic state trajectory terms and $()'$ to denote the perturbation variables terms.

For Eq. (44), the corresponding tangent linear formula is

$$(P_{k+1/2})' = \kappa \frac{\left(\frac{\{p_{k+1/2}\}}{\{p_0\}}\right)^{\kappa}}{\{p_{k+1/2}\}} (p_{k+1/2})' \tag{78}$$

For Eq. (45),

$$\begin{aligned}
(P_k)' = \quad & \frac{1}{1+\kappa}\left[\{p_{k+1/2}\} - \{p_{k-1/2}\}\right]^{-1} \\
& \left[\{p_{k+1/2}\}(P_{k+1/2})' - \{p_{k-1/2}\}(P_{k-1/2})'\right] \\
+ \quad & \frac{1}{1+\kappa}\left[\{p_{k+1/2}\} - \{p_{k-1/2}\}\right]^{-2}\left(\{P_{k-1/2}\} - \{P_{k+1/2}\}\right) \\
& \left[\{p_{k-1/2}\}(p_{k+1/2})' - \{p_{k+1/2}\}(p_{k-1/2})'\right]
\end{aligned} \tag{79}$$

For Eq. (46),

$$\begin{aligned}(\eta_{i,k-1/2})' - (\eta_{i,k+1/2})' = \quad & \{\beta_k\}\{\theta_k\}(\lambda_i)' \\ + \quad & \{\beta_k\}\{\lambda_i\}(\theta_k)' + \{\theta_k\}\{\lambda_i\}(\beta_k)', \\ & k = i+1, i+2, ..., K-1 \end{aligned} \tag{80}$$

where

$$(\beta_k)' = \frac{c_p}{g}\left[(P_{k+1/2})' - (P_{k-1/2})'\right] \tag{81}$$

For Eqs. (48) and (49), we have

$$\begin{aligned}(\eta_{i,i})' = (\eta_{i,i+1/2})' \quad + \quad & \{\beta_i\}\{\theta_i\}(\lambda_i)' \\ + \quad & \{\beta_i\}\{\lambda_i\}(\theta_i)' + \{\theta_i\}\{\lambda_i\}(\beta_i)', \end{aligned} \tag{82}$$

and

$$(\beta_i)' = \frac{c_p}{g}\left[(P_{i+1/2})' - (P_i)'\right] \tag{83}$$

For Eq. (50),

$$\begin{aligned}(\eta_{i,i})' = \quad & \{\lambda_i\}\sum_{k=K-1}^{i}\left[\{\beta_k\}(\theta_k)' + \{\theta_k\}(\beta_k)'\right] \\ + \quad & (\lambda_i)'\sum_{k=K-1}^{i}\{\beta_k\}\{\theta_k\} \end{aligned} \tag{84}$$

The expression Eq. (55) of liquid water mixing ratio of the detraining air from the $i$th cloud type $l_{i,i}$ can be linearized as

$$\begin{aligned}(l_{i,i})' = \quad & -(q_i^*)' + \{\eta_{i,i}\}^{-1}\Bigg\{(q_K)' \\ + \quad & \sum_{j=K-1}^{i+1}\Bigg(\{q_j\}\left[(\eta_{i,j-1/2})' - (\eta_{i,j+1/2})'\right] \\ + \quad & \left[\{\eta_{i,j-1/2}\} - \{\eta_{i,j+1/2}\}\right](q_j)'\Bigg) \\ + \quad & \left(\{\eta_{i,i}\} - \{\eta_{i,i+1/2}\}\right)(q_i)' \\ - \quad & \{q_i\}(\eta_{i,i+1/2})'\Bigg\} + \{\eta_{i,i}\}^{-2}\Bigg\{\{\eta_{i,i+1/2}\}\{q_i\} - \{q_K\} \\ - \quad & \sum_{j=K-1}^{i+1}\left(\{\eta_{i,j-1/2}\} - \{\eta_{i,j+1/2}\}\right)\{q_j\}\Bigg\}(\eta_{i,i})' \end{aligned} \tag{85}$$

The cloud work function expression Eq. (61) can be linearized as

$$
\begin{aligned}
(A_i)' = \quad & \{\epsilon_{K-1}\}(h_K)' + (\epsilon_{K-1})'\{h_K\} \\
- \quad & \{\epsilon_i\}\{\eta_{i,i+1/2}\}(h_i^*)' \\
- \quad & \{\epsilon_i\}\{h_i^*\}(\eta_{i,i+1/2})' - \{\eta_{i,i+1/2}\}\{h_i^*\}(\epsilon_i)' \\
+ \quad & \sum_{j=K-1}^{k} \Bigg\{ \Big[(\epsilon_{k-1})' + (\mu_k)'\Big] \\
& \Bigg[\{h_K\} + \sum_{j=K-1}^{k} \Big(\{\eta_{i,j-1/2}\} - \{\eta_{i,j+1/2}\}\Big)\{h_j\}\Bigg] \\
+ \quad & \Big[\{\epsilon_{k-1}\} + \{\mu_k\}\Big]\Bigg[(h_K)' \\
+ \quad & \sum_{j=K-1}^{k} \Bigg( \Big(\{\eta_{i,j-1/2}\} - \{\eta_{i,j+1/2}\}\Big)(h_j)' \\
+ \quad & \Big[(\eta_{i,j-1/2})' - (\eta_{i,j+1/2})'\Big]\{h_j\}\Bigg)\Bigg]\Bigg\} \\
- \quad & \sum_{k=K-1}^{i+1} \Bigg\{ \Bigg[(\epsilon_k)'\{\eta_{i,k+1/2}\} + \{\epsilon_k\}(\eta_{i,k+1/2})' \\
+ \quad & (\mu_k)'\{\eta_{i,k-1/2}\} + \{\mu_k\}(\eta_{i,k-1/2})'\Bigg]\{h_k^*\} \\
+ \quad & \Big[\{\epsilon_k\}\{\eta_{i,k+1/2}\} + \{\mu_k\}\{\eta_{i,k-1/2}\}\Big](h_k^*)'\Bigg\}
\end{aligned}
\tag{86}
$$

where

$$
\begin{aligned}
(\epsilon_j)' = \quad & \left[\{P_j\}\left(1+\{\gamma_j\}\right)\right]^{-1}(P_{j+1/2})' - \frac{\{P_{j+1/2}\}}{\{P_j\}^2(1+\{\gamma_j\})}(P_j)' \\
- \quad & \frac{\{P_{j+1/2}\}-\{P_j\}}{\{P_j\}(1+\{\gamma_j\})^2}(\gamma_j)'
\end{aligned}
\tag{87}
$$

and

$$
\begin{aligned}
(\mu_j)' = \quad & -\left[\{P_j\}\left(1+\{\gamma_j\}\right)\right]^{-1}(P_{j-1/2})' + \frac{\{P_{j-1/2}\}}{\{P_j\}^2(1+\{\gamma_j\})}(P_j)' \\
+ \quad & \frac{\{P_{j-1/2}\}-\{P_j\}}{\{P_j\}(1+\{\gamma_j\})^2}(\gamma_j)'
\end{aligned}
\tag{88}
$$

The expressions of cumulus effects on the large-scale budgets (Eqs. (70) and (71) are linearized as:

$$
\left(\frac{\partial(\theta_k)'}{\partial t}\right)_c = \quad \frac{\{M_B(i)\}}{c_p\{P_k\}}(\Gamma_s(k))'
$$

$$+ \quad \frac{(M_B(i))'}{c_p\{P_k\}}\{\Gamma_s(k)\} - \frac{\{M_B(i)\}}{c_p\{P_k\}^2}\{\Gamma_s(k)\}(P_k)' \qquad k = 1, 2, ..., K \quad (89)$$

and

$$\left(\frac{\partial(q_k)'}{\partial t}\right)_c = \frac{1}{L}\left\{\{M_B(i)\}\left[(\Gamma_h(k))' - (\Gamma_s(k))'\right] + (M_B(i))'[\{\Gamma_h(k)\} - \{\Gamma_s(k)\}]\right\}, \quad k = 1, 2, ..., K \quad (90)$$

where

$$(\Gamma_s(k))' = \begin{cases} \frac{g}{\{\Delta p_k\}^2}\Big[\{\eta_{i,k-1/2}\}\left(\{s_{k-1/2}\} - \{s_k\}\right) \\ \quad +\{\eta_{i,k+1/2}\}\left(\{s_k\} - \{s_{k+1/2}\}\right) \\ \quad -\{\eta_{i,i}\}\{l_{i,i}\}L\left(1 - \{r_i\}\right)\delta_i^k\Big](\Delta p_k)' \\ +\frac{g}{\{\Delta p_k\}}\Big[\{\eta_{i,k-1/2}\}\left((s_{k-1/2})' - (s_k)'\right) \\ \quad +(\eta_{i,k-1/2})'\left(\{s_{k-1/2}\} - \{s_k\}\right) \\ \quad +\{\eta_{i,k+1/2}\}\left((s_k)' - (s_{k+1/2})'\right) \\ \quad +(\eta_{i,k+1/2})'\left(\{s_k\} - \{s_{k+1/2}\}\right) \\ \quad -\{\eta_{i,i}\}(l_{i,i})'L\left(1 - \{r_i\}\right)\delta_i^k \\ \quad -(\eta_{i,i})'\{l_{i,i}\}L\left(1 - \{r_i\}\right)\delta_i^k \\ \quad +L\{\eta_{i,i}\}\{l_{i,i}\}(r_i)'\delta_i^k\Big], & k = i, i+1, ..., K, \\ 0, & k = 1, 2, ..., i-1 \end{cases} \quad (91)$$

and

$$
(\Gamma_h(k))' = \begin{cases}
\frac{g}{\{\Delta p_k\}^2}\Big[\{\eta_{i,k-1/2}\}\Big(\{h_{k-1/2}\}-\{h_k\}\Big) \\
\quad +\{\eta_{i,k+1/2}\}\Big(\{h_k\}-\{h_{k+1/2}\}\Big) \\
\quad +\{\eta_{i,i}\}\Big(\{h_i^*\}-\{h_i\}\Big)\delta_i^k\Big](\Delta p_k)' \\
+\frac{g}{\{\Delta p_k\}}\Big[\{\eta_{i,k-1/2}\}\Big((h_{k-1/2})'-(h_k)'\Big) \\
\quad +(\eta_{i,k-1/2})'\Big(\{h_{k-1/2}\}-\{h_k\}\Big) \\
\quad +\{\eta_{i,k+1/2}\}\Big((h_k)'-(h_{k+1/2})'\Big) \\
\quad +(\eta_{i,k+1/2})'\Big(\{h_k\}-\{h_{k+1/2}\}\Big) \\
\quad -\{\eta_{i,i}\}\Big((h_i^*)'-(h_i)'\Big)\delta_i^k \\
\quad -(\eta_{i,i})'\Big(\{h_i^*\}-\{h_i\}\Big)\delta_i^k\Big], & k=i,i+1,...,K, \\
0, & k=1,2,...,i-1
\end{cases} \tag{92}
$$

Finally, the cloud work function kernel and cloud-base mass flux expressions Eqs. (74) and (76), respectively, can be linearized as

$$
\begin{aligned}
(K_{i,i})' = \quad & \Big(\{\epsilon_{K-1}\}+\{\vartheta\}\Big)(\Gamma_h(K))'+\Big((\epsilon_{K-1})'+(\vartheta)'\Big)\{\Gamma_h(K)\} \\
- \quad & \Big(\{\epsilon_i\}(\eta_{i,i+1/2})'+(\epsilon_i)'\{\eta_{i,i+1/2}\}+\{\vartheta\}(\eta_{i,i})'+(\vartheta)'\{\eta_{i,i}\}\Big) \\
& \times\Big(1+\{\gamma_i\}\Big)\{\Gamma_s(i)\}-\Big(\{\epsilon_i\}\{\eta_{i,i+1/2}\}+\{\vartheta\}\{\eta_{i,i}\}\Big)(\gamma_i)'\{\Gamma_s(i)\} \\
- \quad & \Big(\{\epsilon_i\}\{\eta_{i,i+1/2}\}+\{\vartheta\}\{\eta_{i,i}\}\Big)\Big(1+\{\gamma_i\}\Big)(\Gamma_s(i))' \\
+ \quad & \sum_{k=K-1}^{i+1}\Bigg\{\Big(\{\epsilon_{k-1}\}+\{\mu_k\}\Big)\Bigg[(\Gamma_h(K))' \\
+ \quad & \sum_{j=K-1}^{k}\Bigg[\Big(\{\eta_{i,j-1/2}\}-\{\eta_{i,j+1/2}\}\Big)(\Gamma_h(j))' \\
+ \quad & \Big((\eta_{i,j-1/2})'-(\eta_{i,j+1/2})'\Big)\{\Gamma_h(j)\}\Bigg]\Bigg] \\
+ \quad & \Big((\epsilon_{k-1})'+(\mu_k)'\Big)\Bigg[\{\Gamma_h(K)\} \\
+ \quad & \sum_{j=K-1}^{k}\Big(\{\eta_{i,j-1/2}\}-\{\eta_{i,j+1/2}\}\Big)\{\Gamma_h(j)\}\Bigg] \\
+ \quad & \{\vartheta\}\Big(\{\eta_{i,k-1/2}\}-\{\eta_{i,k+1/2}\}\Big)(\Gamma_h(k))'
\end{aligned}
$$

$$
\begin{aligned}
&+ \quad \{\vartheta\}\left((\eta_{i,k-1/2})' - (\eta_{i,k+1/2})'\right)\{\Gamma_h(k)\} \\
&+ \quad (\vartheta)'\left(\{\eta_{i,k-1/2}\} - \{\eta_{i,k+1/2}\}\right)\{\Gamma_h(k)\}\Big\} \\
&+ \quad \{\vartheta\}\left(\{\eta_{i,i}\} - \{\eta_{i,i+1/2}\}\right)(\Gamma_h(i))' \\
&+ \quad (\vartheta)'\left(\{\eta_{i,i}\} - \{\eta_{i,i+1/2}\}\right)\{\Gamma_h(i)\} \\
&+ \quad \{\vartheta\}\left((\eta_{i,i})' - (\eta_{i,i+1/2})'\right)\{\Gamma_h(i)\} \\
&- \quad \sum_{k=K-1}^{i+1}\Big\{\Big((\epsilon_k)'\{\eta_{i,k+1/2}\} + \{\epsilon_k\}(\eta_{i,k+1/2})' \\
&+ \quad \{\mu_k\}(\eta_{i,k-1/2})' + (\mu_k)'\{\eta_{i,k-1/2}\}\Big)(1+\{\gamma_k\})\{\Gamma_s(k)\} \\
&+ \quad \Big(\{\epsilon_k\}\{\eta_{i,k+1/2}\} + \{\mu_k\}\{\eta_{i,k-1/2}\}\Big)(\gamma_k)'\{\Gamma_s(k)\} \\
&+ \quad \Big(\{\epsilon_k\}\{\eta_{i,k+1/2}\} + \{\mu_k\}\{\eta_{i,k-1/2}\}\Big)(1+\{\gamma_k\})(\Gamma_s(k))'\Big\}
\end{aligned} \tag{93}
$$

and

$$
(M_B(i))' = \left(\frac{d\{A_i\}}{dt}\right)_{ls}\{K_{i,i}\}^{-2}(K_{i,i})' - \left(\frac{d(A_i)'}{dt}\right)_{ls}\{K_{i,i}\}^{-1} \tag{94}
$$

where

$$
\begin{aligned}
(\vartheta)' = \quad & -\{\epsilon_i\}\{h_i^*\}(\eta_{i,i+1/2})' - (\epsilon_i)'\{h_i^*\}\{\eta_{i,i+1/2}\} - \{\epsilon_i\}(h_i^*)'\{\eta_{i,i+1/2}\} \\
&+ \quad \sum_{k=K-1}^{i+1}\Big\{\Big(\{\epsilon_{k-1}\} + \{\mu_k\}\Big) \\
&\qquad \Big[\sum_{j=K-1}^{k}\Big[\{\eta_{i,j-1/2}\} - \{\eta_{i,j+1/2}\}\Big](h_j)' \\
&+ \quad \Big((\eta_{i,j-1/2})' - (\eta_{i,j+1/2})'\Big)\{h_j\}\Big] \\
&+ \quad \Big((\epsilon_{k-1})' + (\mu_k)'\Big)\Big[\sum_{j=K-1}^{k}\Big(\{\eta_{i,j-1/2}\} - \{\eta_{i,j+1/2}\}\Big)\{h_j\}\Big]\Big\} \\
&- \quad \sum_{k=K-1}^{i+1}\Big[\Big(\{\epsilon_k\}(\eta_{i,k+1/2})' + (\epsilon_k)'\{\eta_{i,k+1/2}\} \\
&+ \quad \{\mu_k\}(\eta_{i,k-1/2})' + (\mu_k)'\{\eta_{i,k-1/2}\}\Big)\{h_k^*\} \\
&+ \quad \Big(\{\epsilon_k\}\{\eta_{i,k+1/2}\} + \{\mu_k\}\{\eta_{i,k-1/2}\}\Big)(h_k^*)'\Big] \\
&+ \quad \{\epsilon_i\}(h_i^*)' + (\epsilon_i)'\{h_i^*\}
\end{aligned}
$$

$$\sum_{k=K-1}^{i+1}\left[\Big(\{\epsilon_k\}+\{\mu_k\}\Big)(h_k^*)'+\Big((\epsilon_k)'+(\mu_k)'\Big)\{h_k^*\}\right] \tag{95}$$

## 3.1 Linearized Discrete Dynamical Equations

## 3.2 Coding of the Tangent Linear Model

For coding the tangent linear model, we linearize the original nonlinear forward model code line by line, do loop by do loop and subroutine by subroutine. This amounts to obtain the exact same tangent linear model as by coding directly from the original linearized model dynamical equations.

The tangent linear model is the linearized nonlinear forward model in the vicinity of a basic state which is a model trajectory. Any original code line, we may write it as

$$U = f(\mathbf{X}) \tag{96}$$

where

$$\mathbf{X} = (x_1,\ x_2,\ \cdots,\ x_m)^T \tag{97}$$

and $U$ is a new derived variable related to the original control variables of the nonlinear forward model, i.e., it may be one of the original control variables or an intermediate variable which is a function of the original control variables. Here $x_1,\ x_2,\ \cdots,\ x_m$ (the components of the vector $\mathbf{X}$) are the required variables to derive $U$, which may consist of either the original model control variables or of the intermediate variables derived from the original control variables; $m$ is the number of the required variables.

The corresponding tangent linear code assumes the form:

$$\begin{aligned}\delta U = \quad & \delta x_1\left(\frac{\partial f}{\partial x_1}\right)_{\mathbf{X}=\mathbf{X}_{basic\ state}} + \delta x_2\left(\frac{\partial f}{\partial x_2}\right)_{\mathbf{X}=\mathbf{X}_{basic\ state}} + \cdots + \\ & + \delta x_m\left(\frac{\partial f}{\partial x_m}\right)_{\mathbf{X}=\mathbf{X}_{basic\ state}}\end{aligned} \tag{98}$$

where $\mathbf{X}=\mathbf{X}_{basic\ state}$ means that in the expression $\frac{\partial f}{\partial x_i},\ i=1,\ 2,\ \cdots,\ m$, all the values of the required variables $x_1,\ x_2,\ \cdots,\ x_m$ are chosen to have the exact same values as those of the basic state trajectory as in the nonlinear forward model to ensure that the basic state of the integration of tangent linear model is exactly the basic state of the nonlinear model integrating trajectory. Here $\delta U$ and $\delta x_1,\ \delta x_2,\ \cdots,\ \delta x_m$ are the corresponding perturbation variables of $U$ and $x_1,\ x_2,\ \cdots,\ x_m$, respectively.

In order to obtain the necessary values of $\mathbf{X}_{basic\ state}$, the nonlinear model integrating trajectory, for the tangent linear model, we must apply the parallel method. This method consists of calculating in parallel the nonlinear model trajectory as the basic state $\mathbf{X}_{basic\ state}$ and the integration of perturbation variables as well, such as $\delta U$, in the tangent linear model.

### 3.3 Notational Convention for Variables and Subroutines Used in the Tangent Linear Model Code

For convenience, the same original names used in the nonlinear forward model are employed for the corresponding perturbation variables in the tangent linear model code. For instance, we use "$U$" for "$\delta U$", "$PKHT$" for "$\delta(PKHT)$", "$AKM$" for "$\delta(AKM)$", etc.. This also means that the perturbation control variables in the TLM share the same common structure and same common block names as the full variables of the GCM itself. Thus, one needs to pay attention to this issue when running the TLM in conjunction with the original GCM.

We append a "0" at the end of a variable name in the original nonlinear forward model to represent the corresponding basic state variable, such as "$U0$" for "$U_{basic\ state}$", "$PKHT0$" for "$(PKHT)_{basic\ state}$" , "$AKM0$" for "$(AKM)_{basic\ state}$", etc..

For naming subroutines in the tangent linear model, we simply append a "$L$" at the beginning of the original names of subroutines of the nonlinear forward model. To conform with ANSI FORTRAN 77 language, if the new name of a tangent linear subroutine exceeds six letters, we just retain its first six letters. For instance, the original subroutines of the nonlinear model "$RASG$", "$MOISTIO$" and "$RNEVP$", have corresponding names in the tangent linear model as "$LRASG$", "$LMOIST$" and "$LRNEVP$", respectively.

## 4 Adjoint Model of the Moist Process Physics Package

### 4.1 Using the Adjoint Method to Calculate the Gradient of a Cost Function

The practical determination of the adjoint model of the moist physics package used in NASA GEOS-1 C-Grid GCM is the key computational method enabling us to calculate the gradient of a cost function with respect to initial conditions (or other control variables) for carrying out a 4-D variational assimilation. In 4-D variational assimilation, the cost function, which measures the weighted difference between observations and forecasts in an adequate norm, is minimized by using a large-scale unconstrained minimization method iteratively which requires for its implementation the gradient of the cost function with respect to the control variables. Finally, the optimal state defines a trajectory which passes as close as possible in a least-squares sense to the observations while satisfying the system of coupled partial differential equations of the numerical weather prediction model as strong constrains.

Assuming that the cost function consists of a weighted least square fit of the model forecast

to the observations, it has the form :

$$J(\mathbf{X}(t_0)) = \frac{1}{2}\sum_{r=0}^{R}\left(\mathbf{X}(t_r) - \mathbf{X}^{obs}(t_r)\right)^T \mathbf{W}(t_r)\left(\mathbf{X}(t_r) - \mathbf{X}^{obs}(t_r)\right) \tag{99}$$

where $\mathbf{X}(t_r)$ is a model state vector of size $M(4K+1)$ containing the values of the zonal wind $u$, the meridional wind $v$, the potential temperature $\theta$, the surface pressure $P_s$, and the surface humidity $q$; here $M$ is the number of grid points at each level; $K$ is number of vertical levels. $t_r$ is a given time in the assimilation window; $\mathbf{X}^{obs}(t_r)$ is a vector of observations defined over all grid points on all levels at time $t_r$; $\mathbf{W}(t_r)$ is an $N \times N$ diagonal weighting matrix. From Navon et al. (1992), we have the following expression

$$\left(\nabla J\left(\mathbf{X}(t_0)\right)\right)^T \mathbf{X}'(t_0) = \sum_{r=0}^{R}\left(\mathbf{W}(t_r)\left(\mathbf{X}(t_r) - \mathbf{X}^{obs}(t_r)\right)\right)^T \mathbf{X}'(t_r). \tag{100}$$

where $\mathbf{X}'(t_0)$ is the initial perturbation, $\mathbf{X}'(t_r)$ is the perturbation in the forecast resulting from the initial perturbation, $\nabla J\left(\mathbf{X}(t_0)\right)$ is the gradient of the cost function with respect to the initial conditions.

The tangent linear model of the nonlinear forward model can be symbolically expressed as

$$\mathbf{X}'(t_r) = \mathbf{P}_r \mathbf{X}'(t_0) \tag{101}$$

where $\mathbf{P}_r$ represents the result of applying all the operator matrices in the linear model to obtain $\mathbf{X}'(t_r)$ from $\mathbf{X}'(t_0)$.

We define the adjoint model as

$$\hat{\mathbf{X}}^r(t_0) = \mathbf{P}_r^T \hat{\mathbf{X}}(t_r), \quad r = 1, \cdots, R, \tag{102}$$

where $\hat{(\,)}$ represents an adjoint variable. After some algebra we obtain (see Navon et al. 1992) that the expression for the gradient of the cost function with respect to the initial condition is

$$\nabla J\left(\mathbf{X}(t_0)\right) = \sum_{r=0}^{R} \mathbf{P}_r^T \mathbf{W}(t_r)\left(\mathbf{X}(t_r) - \mathbf{X}^{obs}(t_r)\right) \tag{103}$$

From this analysis, we note that the so called adjoint model operator is just the transpose of the tangent linear model operator.

## 4.2 Coding of the Adjoint Model

Since the adjoint model equations consist of the transpose of the linearized version of the nonlinear forward model, if we view the tangent linear model as the result of the multiplication of a number of operator matrices:

$$\mathbf{P} = \mathbf{A}_1 \mathbf{A}_2 \cdots \mathbf{A}_N, \tag{104}$$

where each matrix $\mathbf{A}_i (i = 1, \cdots, N)$ represents either a subroutine or a single $DO$ loop, then the adjoint model can be viewed as being a product of adjoint subproblems

$$\mathbf{P}^T = \mathbf{A}_N^T \mathbf{A}_{N-1}^T \cdots \mathbf{A}_1^T. \tag{105}$$

Thus, the adjoint model is simply the complex conjugate of all the operations in the tangent linear model. Each DO loop or each subroutine in the tangent linear model has its adjoint image DO loop and subroutine, respectively. Therefore, we code the adjoint model directly from the discrete tangent linear model by rewriting the code of the tangent linear model statement by statement in the opposite direction. This simplifies not only the complexity of constructing the adjoint model but also avoids the inconsistency generally arising from the derivation of the adjoint equations in analytic form followed by the discrete approximation (due to non-commutativity of discretization and adjoint operations).

## 4.3 Notational Convention for Variables and Subroutines Used in the Adjoint Model Code

In a similar way as in the tangent linear model, we employed the same original variable names used in the nonlinear forward model for the corresponding adjoint variables in the adjoint model code. For instance, we use "$U$" for "$\hat{U}$", "$PKHT$" for "$(\widehat{PKHT})$", "$AKM$" for "$(\widehat{AKM})$", etc.. As in the TLM, this convention also means that the adjoint control variables in the adjoint model share the same common structure and same common block names as the GCM itself. Thus, one needs to pay attention to it when running the adjoint in conjunction with the original GCM.

We also just append a "0" at the end of a variable name (in a similar way as done previously in the tangent linear model) to represent the corresponding basic state variable, such as using "$U0$" for "$U_{basic\ state}$", "$PKHT0$" for "$(PKHT)_{basic\ state}$", "$AKM0$" for "$(AKM)_{basic\ state}$", etc., needed in the adjoint code.

For naming subroutines, we simply change the letter "$L$" at the beginning of the names of the tangent linear model subroutines to "$A$" and used them as corresponding adjoint model subroutine names. We also retain the adjoint subroutine names which do not exceed six letters to conform with ANSI FORTRAN 77 language. For instance, the original subroutines of the nonlinear model "$RASG$", "$MOISTIO$" and "$RNEVP$", have corresponding names in the adjoint model as "$ARASG$", "$AMOIST$" and "$ARNEVP$", respectively.

## 4.4 Verification of the Correctness of the Adjoint Model

Integrating the nonlinear model forward in time and its adjoint backwards in time, while forcing the r.h.s.of the adjoint model with difference between model and observations (see

Eq. (103)), one can obtain values for the gradient of cost function with respect to distributed control variables, which may consist of either the initial conditions or the initial conditions plus boundary conditions or model parameters. Since the moist version of NASA GEOS-1 C-Grid GCM consists of thousands of lines of code, any minor coding error may cause the final gradient of cost function with respect to the control variables to be erroneous. Therefore, we need to verify the correctness of the linearization and adjoint coding segment by segment. Each segment may consist of either a subroutine or of several DO loops. For a detailed derivation of the adjoint model and verification of its correctness, see Navon et al. (1992).

The correctness of the adjoint of each operator was checked by applying the following identity (Navon et al. 1992)

$$(AQ)^{*T}(AQ) = Q^{*T}\left(A^{*T}(AQ)\right), \tag{106}$$

where $Q$ represents the input of the original code, $A$ represents either a single $DO$ loop or a subroutine. The left hand side involves only the tangent linear code, while the right hand side involves also adjoint code ($A^{*T}$). If equality (106) holds, the adjoint code is correct when compared with the TLM. In practice the identity Eq. (106) holds only up to machine accuracy. In our verifications of the correctness of each segment of the adjoint model and the whole adjoint model, the LHS and the RHS of Eq. (106) attained 13 digits of accuracy which is near the machine precision limit. The test were performed at NASA's Cray C-90 computer which has intrinsic double precision. These results show that our adjoint code consists of absolutely the exact adjoint operators of the TLM of the moist version of NASA GEOS-1 C-Grid GCM.

A gradient check (Figs. 1, 2) was then performed to assess accuracy of the discrete adjoint model. This verification method is described next. First, we chose the cost function $J$ as in Eq. (99) and the $N \times N$ diagonal matrix $W = diag(\mathbf{W}_u, \mathbf{W}_v, \mathbf{W}_\theta, \mathbf{W}_q, \mathbf{W}_{Ps})$, where the diagonal submatrices are defined as : $\mathbf{W}_u = 5 \times 10^{-1}\mathbf{I}$ $s^2m^{-2}$, $\mathbf{W}_v = 5 \times 10^{-1}\mathbf{I}$ $s^2m^{-2}$, $\mathbf{W}_\theta = 10^{-3}\mathbf{I}$ $K^{-2}$, $\mathbf{W}_q = 5 \times 10^{-3}\mathbf{I}$, $\mathbf{W}_{Ps}$= $10^{-3}\mathbf{I}$ $mb{-}2$. Then, let

$$J(\mathbf{X} + \alpha\mathbf{h}) = J(\mathbf{X}) + \alpha\mathbf{h}^T\nabla J(\mathbf{X}) + O(\alpha^2), \tag{107}$$

be a Taylor expansion of the cost function. Here $\alpha$ is a small scalar and $\mathbf{h}$ is a vector of unit length (such as $\mathbf{h} = \nabla J/\|\nabla J\|$). Rewriting the formula above we can define a function of $\alpha$ as

$$\Phi(\alpha) = \frac{J(\mathbf{X} + \alpha\mathbf{h}) - J(\mathbf{X})}{\alpha\mathbf{h}^T\nabla J(\mathbf{X})} = 1 + O(\alpha). \tag{108}$$

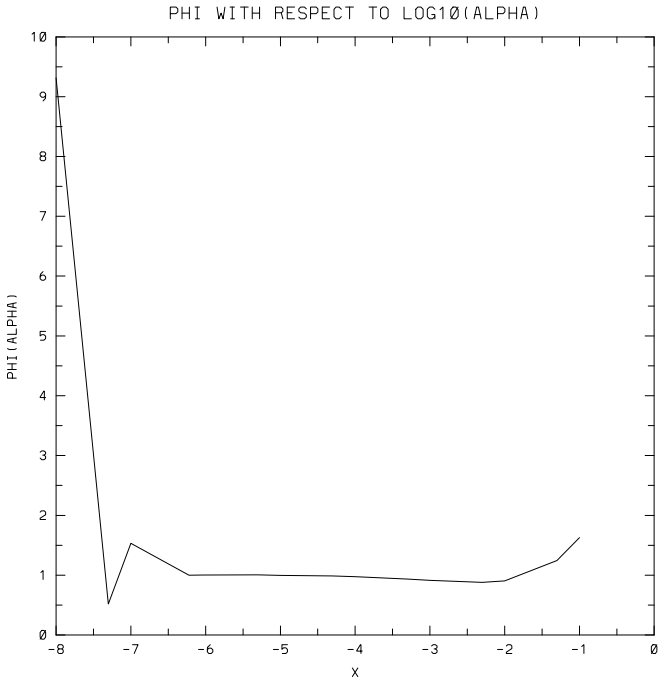


Figure 1: Variation of the $\phi(\alpha)$ with respect to $\log \alpha$ (gradient check of correctness of adjoint model). Integration period is 6 hours and $t = 6$ hours model generated observations were used. January 1, 1985 00Z DAO's data was used as $t = 0$ observations. The first guess is the shifted 6-hour initial condition. The time integration scheme employed is the leapfrog scheme.

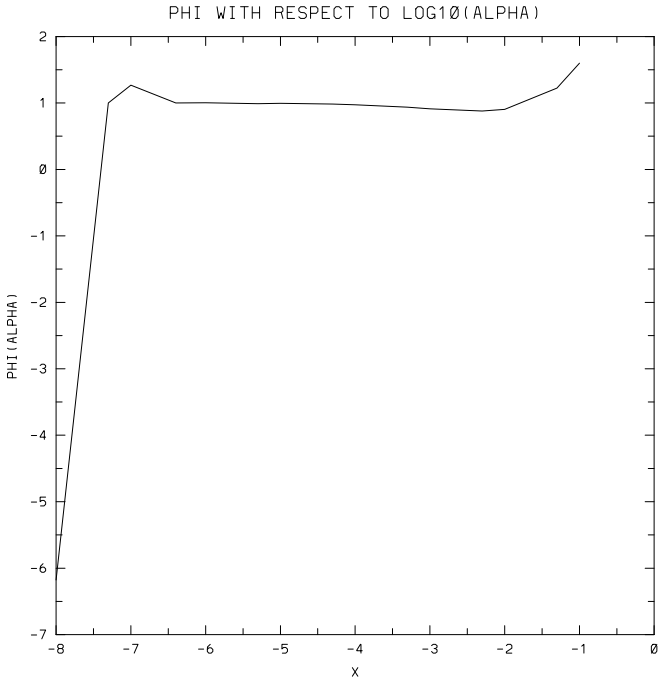


Figure 2: As in Figure 1, but for the Matsuno time integration scheme.

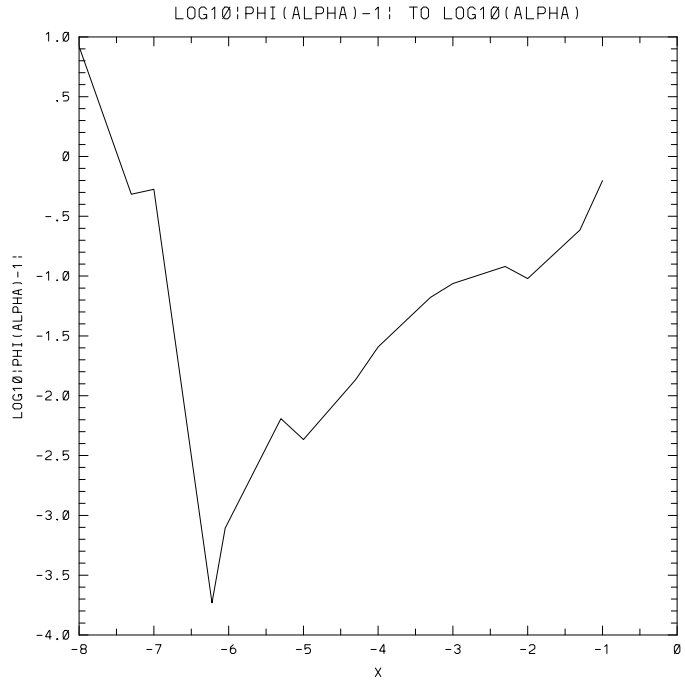


Figure 3: Variation of the $\log|\phi(\alpha)-1|$ with respect to $\log\alpha$. Integration period is 6 hours and $t = 6$ hours model generated observations were used. January 1, 1985 00Z DAO's data is used as $t = 0$ observations. The first guess is the shifted 6-hour initial condition. The time integration scheme employed is the leapfrog scheme.

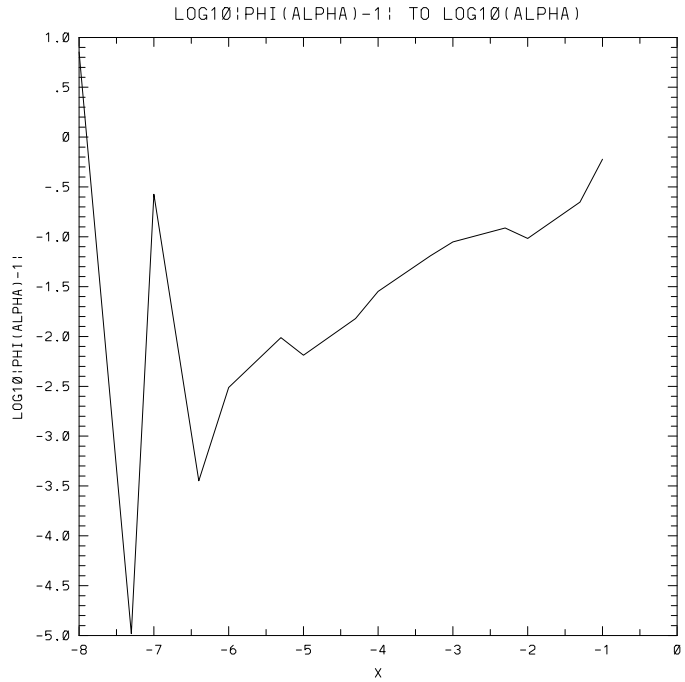


Figure 4: As in Figure 3, but for the Matsuno time integration scheme.

For values of $\alpha$ which are small but not too close to the machine zero, one should expect to obtain values for $\Phi(\alpha)$ which are close to unity. We obtained values for the function $\phi(\alpha)$ equal unity to a high degree of accuracy when the parameter $\alpha$ is varied from $10^{-2}$ to $10^{-6}$. From the residual of $\phi(\alpha)$ (Figs. 3, 4), we found that the residual tends to zero. The gradient check verifies that the adjoint model is correct and can be used, for example, to perform 4-D VDA experiments.

Although the gradient check results are good, comparing the gradient check results with those for the adiabatic version of the NASA GEOS-1 GCM (Yang and Navon 1996), we find that including moist processes into the GCM decrease the validity of the tangent linear approximation. It worsens both in terms of the accuracy of the gradient values of the cost functional as well as in the range of the perturbations, in which satisfactory values of the gradient of the cost functional are maintained. The reasons are:

1) The high nonlinearity of the original moist process package including the RAS cumulus parameterization and large-scale precipitation and evaporation scheme. Since the Arakawa-Schubert parameterization is the most complex cumulus convective parameterization scheme which provides the most complete physics approach and has an inherent iterative feature, the nonlinearity of the AS scheme as well as the RAS scheme is much stronger than that of some other moist parameterization schemes, such as Kuo's scheme.

2) In AS and RAS, the on-off discontinuous effects are more pronounced than in other types of moist parameterization schemes. This is due to the fact that there are more on-off switch processes used in Arakawa-Schubert type scheme and the iterative feature of the AS parameterization. Obviously these discontinuities worsen the validity of the tangent linear approximation and cause the values of the calculated gradient of the cost functional to exhibit jumps.

Several research efforts were presented related to the serious influence of the on-off switch processes on the validity of the tangent linear approximation. For instance, Vukicevic and Errico (1993) tested the accuracy of the tangent linear model of a mesoscale model, compared the "true" perturbation obtained by direct nonlinear integration and concluded that significant errors may be expected in the regions where the moist diabatic processes are important for finite perturbations in the initial conditions. Recently, both Bao and Kuo (1995) and Xu (1996) carried out a detailed study using idealized continuous examples with delta function mimicking the on-off switches in physical schemes. They indicated that ignoring the variation of the switch point due to the perturbation in the initial conditions, i.e., keeping the switching point in the tangent linear model the same as in the basic state, could cause significant errors in the tangent linear model solution and gradient calculation. Thus how to deal with the on-off switches used in the moist process parameterization is a crucial issue.

The essence of the influence of on/off discontinuous processes is that they may cause sudden jumps in the model integration trajectories, these jumps changing the model trajectories

and forcing the value of the cost function and its gradient to undergo a sudden change. This sudden change is equivalent to introducing a high nonlinearity into the variational assimilation system. As a consequence, it may cause either a failure or a slow-down of the minimization processes in 4-D Var. Simply smoothing the parameterization at the discontinuous points such as tested by (Zupanski 1993; Tsuyuki 1996a, b, c) cannot completely remove the influence of on/off discontinuous. Also the simple smoothing method may introduce a negative effect: that of changing the character of the original parameterization system.

3) Truncation errors may worsen the validity of the tangent linear approximation. In the original code of the RAS scheme, there are some computational steps involving processes whereby a very small output results from the difference between two very large terms whose values are of similar magnitude, such as in calculating the rate of change of large-scale variables by the forcing of cumulus-scale processes. These very small time tendency terms result from the difference between two corresponding variable terms. Besides, a nonlinear term involving $N$ dependent variables in the nonlinear forward model will create $N$ terms in tangent linear computations. These newly created computation processes may increase the truncation error. We have checked the validity of the tangent linear approximation term by term and line by line in the tangent linear model, and found that the truncation error is a contributing factor towards a reduction in the range of validity of the tangent linear approximation.

## Acknowledgments

This work has been supported by NASA-Grant NAG 5-1660 managed by Dr. Ken Bergman, Section Head, Climate Modeling.

## References


Arakawa, A., 1969: Parameterization of cumulus convection, *Proc. WMO/IUGG Symp. Numerical Weather Prediction*, Tokyo, 20 November-4 December, 1968, Japan Meteorology Agency, IV, 8, 1-6.

Arakawa, A., 1971: A parameterization of cumulus convection and its application to numerical simulation of the tropical general circulation Paper presented at the *7th Tech. Conf. on Hurricanes and Tropical Meteorology*, Barbados, Amer. Meteor. Soc.

Arakawa, A., 1972: Parameterization of cumulus convection, Design of the UCLA general circulation model, Numerical simulation of weather and climate, *Tech. Rept. 7*, Dept. of Meteorology, University of California, Los Angeles.

Arakawa, A., and M. J. Suarez, 1983: Vertical Differencing of the Primitive Equations in sigma coordinates, *Mon. Wea. Rev.*, **111**, 34-45.

Arakawa, A., and W. H. Schubert, 1974: Interaction of a cumulus cloud ensemble with the large-scale environment, Part I, *J. Atmos. Sci.*, **31**, 674-701.

Bao, J.-W., and Y.-H. Kuo, 1995: On-off switches in the adjoint method: step functions, *Mon. Wea. Rev.*, **123**, 1589-1594.

Betts, A. K., 1973a: Nonprecipitating cumulus convection and its parameterization, *Quart. J. Roy. Meteor. Soc.*, **99**, 178-196.

Betts, A. K., 1973b: A composite mesoscale cumulonimbus budget, *J. Atmos. Sci.*, **30**, 597-610.

Caselski, B. F., 1974: Cumulus convection in weak and strong tropical disturbances, *J. Atmos. Sci.*, **31**, 1241-1255.

Charney, J. G., and A. Eliassen, 1964: On the growth of the hurricane depression, *J. Atmos. Sci.*, **21**, 68-75.

Fraedrich, K., 1973: On the parameterization of cumulus convection by lateral mixing and compensating subsidence, Part 1, *J. Atmos. Sci.*, **30**, 408-413.

Gray, W. M., 1972: Cumulus convection and large-scale circulations, Part III. Broad scale and meso scale considerations, *Atmos. Sci. Paper No. 190*, Colorado State University, 80 pp.

Hack, J. J., W. H. Schubert, and P. L. Silva Dias, 1984: A spectral cumulus parameterization for use in numerical models of the tropical atmosphere, *Mon. Wea. Rev.*, **112**, 704-716.

Kao, C.-Y., and Y. Ogura, 1987: Response of cumulus clouds to large-scale forcing using the Arakawa-Schubert cumulus parameterization, *J. Atmos. Sci.*, **44**, 2437-2458.

Koster, R. D., and M. J. Suarez, 1992: Modeling the land surface boundary in climate models as a composite of independent vegetation stands, *J. Geophys. Res.*, **97**, 2697-2715.

Koster, R. D., and M. J. Suarez, 1996: Energy and water balance calculations in the Mosaic LSM, *NASA Technical Memorandum 104606*, **Vol. 9**, Technical Report Series on Global Modeling and Data Assimilation, Max J. Suarez, Editor.

Kuo, H. L., 1965: On the formation and intensification of tropical cyclones through latent heat release by cumulus convection, *J. Atmos. Sci.*, **22**, 40-63.

Kuo, H. L., 1974: Further studies of the parameterization of the influence of cumulus convection on large-scale flow, *J. Atmos. Sci.*, **31**, 1232-1240.

Krishnamurti, T. N., 1969: An experiment in numerical prediction in equatorial latitudes, *Quart. J. Roy. Meteor. Soc.*, **95**, 594-620.

Krishnamurti, T. N., H. Pan, C. B. Chang, J. Ploshay, and W. Oodaly, 1979: Numerical weather prediction for GATE, *Quart. J. Roy. Meteor. Soc.*, **105**, 979-1010.

Krishnamurti, T. N., Y. Ramanathan, H.-L. Pan, R. J. Pasch, and J. Molinari, 1980: Cumulus parameterization and rainfall rates I, *Mon. Wea. Rev.*, **108**, 465-472.

Lilly, D. K., 1960: On the theory of disturbances in a conditionally unstable atmosphere, *Mon. Wea. Rea.*, **88**, 1-17.

López, R. E., 1972a: Cumulus convection and large scale circulations, Part I. A parameteric model of cumulus convection, *Atmos. Sci. Paper No. 188*, Colorado State University, 100 pp.

López, R. E., 1972b: Cumulus convection and large scale circulations, Part II. Cumulus and meso scale considerations, *Atmos. Sci. Paper No. 189*, Colorado State University, 63 pp.

Lord, S. J., and A. Arakawa, 1980: Interaction of a cumulus cloud ensemble with the large-scale environment, Part II, *J. Atmos. Sci.*, **37**, 2677-2692.

Lord, S. J., 1982: Interaction of a cumulus cloud ensemble with the large-scale environment, Part III: Semi-prognostic test of the Arakawa-Schubert Cumulus Parameterization, *J.*

*Atmos. Sci.*, **39**, 88-103.

Lord, S. J., W. C. Chao, and A. Arakawa, 1982: Interaction of a cumulus cloud ensemble with the large-scale environment, Part IV: The discrete model, *J. Atmos. Sci.*, **39**, 104-113.

Manabe, S., J. Smagorinsky, and R. F. Strickler, 1965: Simulated climatology of a general circulation model with a hydrologic cycle, *Mon. Wea. Rev.*, **93**, 769-798.

Moorthi, S., and A. Arakawa, 1985: Baroclinic instability with cumulus heating, *J. Atmos. Sci.*, **42**, 2007-2031.

Moorthi, S., and M. J. Suarez, 1992: Relaxed Arakawa-Schubert: A parameterization of moist convection for general circulation models, *Mon. Wea. Rev.*, **120**, 978-1002.

Navon, I. M., X. Zou, J. Derber, and J. Sela, 1992: Variational data assimilation with an adiabatic version of the NMC spectral model. *Mon. Wea. Rev.*, **120**, 1433-1446.

Ooyama, K., 1964: A dynamical model for the study of tropical cyclone development, *Geofis. Inst.*, **4**, 187-198.

Ooyama, K., 1969: Numerical simulation of the life cycle of tropical cyclones, *J. Atmos. Sci.*, **26**, 3-40.

Ooyama, K., 1971: A theory on parameterization of cumulus convection, *J. Meteor. Soc. Japan*, **49**, 744-756.

Phillips, N. A., 1974: Application of Arakawa's energy conserving layer model to operational numerical weather prediction, *Office Note 104, National Meteorological Center*, NWS/NOAA, 40 pp.

Ramanathan, Y., 1980: Cumulus Parameterization in a case study of a monsoon depression, *Mon. Wea. Rev.*, **108**, 313-321.

Vukićević, T., and R. M. Errico, 1993: Linearization and adjoint of parameterized moist diabatic process, *Tellus*, **45A**, 493-510.

Schubert, S. D., J. Pfaendtner, and R. Rood, 1993: An assimilated data set for Earth Science applications, *Bull. Ameri. Meteor. Soc.*, **74**, 2331-2342.

Silva-Dias, P. L., and W. H. Schubert, 1977: Experiments with a spectral cumulus parameterization theory, *Atmos. Sci. Pap.*, **No. 275**, Colorado State University, 132 pp..

Suarez, M. J., and L. L. Takacs, 1995: Documentation of the ARIES/GEOS Dynamical

Core, Version 2, *NASA Technical Memorandum 104606*, **Vol. 5**, Technical Report Series on Global Modeling and Data Assimilation, Max J. Suarez, Editor, April 1995.

Sud, Y., and A. Molod, 1988: The roles of dry convection, cloud-radiation feedback processes and the influence of recent improvements in the parameterization of convection in the GLA GCM, *Mon. Wea. Rev.*, **116**, 2366-2387.

Sud, Y. C., W. C. Chao, and G. K. Walker, 1991: Contributions to the implementation of the Arakawa-Schubert cumulus parameterization in the GLA GCM, *J. Atmos. Sci.*, **48**, 1573-1586.

Takacs, L. L., A. Molod, and T. Wang, 1994: Goddard Earth Observing System (GEOS) General Circulation Model (GCM), Version 1, *NASA Technical Memorandum 104606*, **Vol. 1**, Technical Report Series on Global Modeling and Data Assimilation, Max J. Suarez, Editor, September 1994.

Tiedtke, M., 1989: A comprehensive mass flux scheme for cumulus parameterization in large-scale models, *Mon. Wea. Rev.*, **117**, 1779-1800.

Tsuyuki, T., 1996a: Variational data assimilation in the tropics using precipitation data, part I: Column model, *Meteorology and Atmospheric Physics*, **60**, 87-104.

Tsuyuki, T., 1996b: Variational data assimilation in the tropics using precipitation data, part II: 3-D model, *Mon. Wea. Rev.*, **124**, 2545-2561.

Tsuyuki, T., 1996c: Variational data assimilation in the tropics using precipitation data, part III: Assimilation of SSM/I precipitation rates, Submitted to *Mon. Wea. Rev.*.

Xu, Q., 1996: Generalized adjoint for physical processes with parameterized discontinuities, Part I: Basic issues and heuristic examples, *J. Atmos. Sci.*, **53**, 1123-1142.

Yanai, M., 1964: Formation of tropical cyclones, *Rev. Geophys.*, **2**, 367-414.

Yanai, M., 1971a: A review of recent studies of tropical meteorology relevant to the planning of GATE, *Experimental Design Proposal by the Interim Scientific and Management Group (ISMG)*, WMO, Vol.**2**, Annex I, 1-43.

Yanai, M., 1971b: The mass, heat and moisture budgets and the convective heating within tropical cloud clusters, Paper presented at the *7th Tech. Conf. on Hurricanes and Tropical Meteorology*, Barbados, Amer. Meteor. Soc..

Yanai, M., S. Esbensen, and J.-H. Chu, 1973: Determination of bulk properties of tropical cloud clusters from large scale heat and moisture budgets, *J. Atmos. Sci.*, **30**, 611-627.

Yang, W., and I. M. Navon, 1995: Documentation of the tangent linear model and its

adjoint of the adiabatic version of the NASA GEOS-1 C-grid GCM - version 5.2, *Technical Report*, **FSU-SCRI-95T-52**, Supercomputer Computations Research Institute, Florida State University, 60 pp.

Yang, W., and I. M. Navon, 1995: Documentation of the tangent linear model and its adjoint of the adiabatic version of the NASA GEOS-1 C-grid GCM - version 5.2, *NASA Technical Memorandum*, **No. 104606, Vol. 8**, Technical Report Series on Global Modeling and Data Assimilation, Max J. Suarez, Editor, March 1996; Also available at http://dao.gsfc.nasa.gov/subpages/tech-reports.html, Volume 8.

Županski, D., 1993: The effects of discontinuities in the Betts-Miller cumulus convection scheme on four-dimensional variational data assimilation, *Tellus*, **45A**, 511-524.